Analysis of the Noise and Vibration of a Dry Screw Compressor

Overview of structural and torsional resonance, Identification of torque peak increase at input shaft in the drive train, free and forced torsional models development using the Holzer method, sensitivity analyses of critical parameters to determine weakest link in drive train, gear backlash and associated noise in the drive train

Dr.-Ing. J. Willie,
Dipl.-Ing.(FH) W. Asal,
Dr.-Ing. R. Sachs,
Gardner Denver Schopfheim GmbH

Abstract

Screw compressors are very common in industry and their torsional vibration behavior is very important. When this issue is neglected in the design it can lead to torsional resonance in the machine during operation. This is especially true if the structural integrity of the machine does not take this into account in the design. This phenomenon has been reported in most of these machines and the excitation or modulation is usually provided by the drive. It can lead to high torque peak fluctuation in the drive shaft and in the worst case to fatigue failure. Its prevention has to be taken into consideration during the construction of the machine. It is important to find out how the internals of such machines respond to torsional vibration modes and whether their modification can shift such modes.

This paper presents torsional vibration analyses of screw compressors, which are designed oil free for mounting on trucks for year round use and tested at Gardner Denver (GD). Measurements at test stands and field test show that the torque peak in the drive shaft can fluctuate and show large values than normal. They also show that the nature of the excitation and hence the response of the machine depends on the drive and the excitation amplitude. To predict this behaviour detailed free and forced torsional models are developed and validated with measurement data. The latter enables the validation of the torque peaks obtained in measurement. The drive train configuration (branched or unbranched) is taken into account and a method that can handle both configurations, the Holzer method, is used. Sensitivity analyses of inertias and stiffness is performed and reported. Based on this the weakest link in the drive train is identified and presented.

1. Introduction

This project was initiated as a result of changes in chassis layout to a 6x2 format for the mobile tanker industry. The compressor is aimed at the dry bulk market which is currently supported by GD XK and BL series machines. Due to the recent changes in chassis layout these existing technologies cannot be packaged inboard on the tractor unit for direct drive applications (See Figure 1). The new compressor design will replace these existing technologies on the new chassis format. However, during initial test the machine is exhibiting vibration when it is run with an electric motor and a diesel engine on test cells at GD. The same is true when the machine is tested on a truck. In all the cases, a significant torque increase is observed at a critical running speed of the compressor. In addition to the torque peak, the compressor shows lateral vibration and an increase in noise levels. The compressor is powered on the truck using a power take off (PTO), which is a mechanism attached to a motor vehicle engine that supplies power to a nonvehicular device, such as a pump or a compressor.

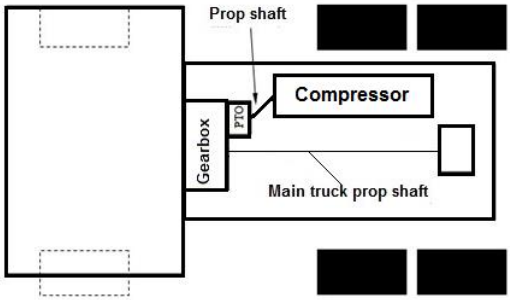

Fig.1: Sketch of truck with mounted compressor and PTO and prop-shaft

There are many sources of pulsation/vibration in compressors. Some include mechanical (torsional/structural), flow induced/process oscillations, speed/dynamic oscillations, reliability/structural integrity issues, to mention but a few. Specifically, sources of pulsation/vibration in screw compressors include the shape of the discharge port, the screw profile, the internal clearances, the internal volume ratio, over compression, and under compression, etc [1]. Pulsation and noise issues are encountered in practice almost on a daily basis. For example, Leader, et al. [2] did a review of torsional resonance cases encountered in industry. They discussed the practical implementation of torsional analysis in real machines. Various cases, for example, synchronous motors, reciprocating engines, compressors and pumps, variable frequency drives (VFDs) and gears are discussed. In [3], a VFD is identified as the source of high torsional vibration in a motor/ID fan system

operating far away from the system natural torsional frequencies. Identification of this type of torsional resonance, which is not classical, during the design, is difficult.

The aim of this work is to understand the sources of the torque peak fluctuation measured at the motor shaft and the noise in the drive train of a screw compressor. Using Finite Element Analysis (FEA), structural modal frequencies of the compressor housing are determined and validated with measurements using hammer test. The same is done for the compressor housing with the mountings of the electric motor. In both cases, the frequencies and mode shapes are close to those obtained in measurements. A field test on a truck is carried out in which the mounting bracket is braced to the ground to significantly increase the structural stiffness of the system and the frequency measured. The truck resonant frequency did not change. As a result, it is concluded that the resonance in the system cannot be structural but torsional. This motivated the work that is presented here. It is divided into the following: An introduction, a brief background of torsional resonance, free and forced torsional models development using the Holzer method for unbranched and branched drive trains, results and discussions and conclusion and future outlook.

2. Torsional resonance background

Drive trains consisting of rotating elements (Gears, shafts connection, etc) can exhibit steady state vibration and when this is the case it is possible to develop torsional models that can be used to predict the natural torsional frequencies of the system.

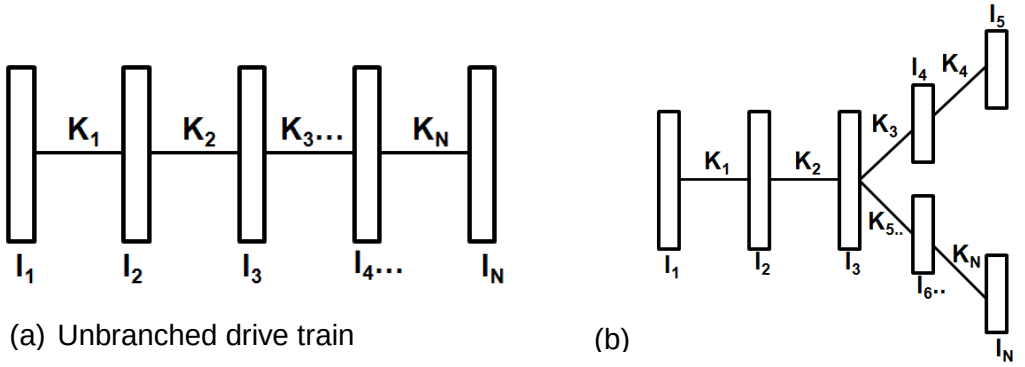

(a) Unbranched drive train (b)

Fig. 2: Schematic of drive train configuration with unbranching and branching

This is done by assuming that each gear is a lumped mass and the shafts connecting them to have torsional stiffness. If the drive train is subjected to external excitation this can also be included and it is referred to as forced torsional vibration. The former is referred to as free torsional vibration. The masses are concentrated at nodal points as shown in Figs. 2(a) and (b). In Fig. 2(a), we do not have two or more shafts in the system branching from a

gear point, which is a branched drive train, whereas in Fig. 2(b), a branched point is in the drive train. In this figure, the inertias, denoted by I and the torsional stiffness, denoted by K, are all speed reduced to the input shaft and so the system is referred to as an equivalent system. This is done by multiplying the inertia and the stiffness by the square of the overall transmission ratio, i.

The general dynamic equation used for analyzing torsional systems can be written as:

$$[I]\{\ddot{\theta}\}+[C]\{\dot{\theta}\}+[K]\{\theta\}=\{T(t)\} \qquad (1)$$

Where I is the inertia matrix, C is the torsional damping matrix, K is the torsional stiffness matrix and T(t) is the forcing torque. To determine the natural torsional frequencies of the system, T(t)=0. In the analysis carried out in this work, damping is neglected, which is known to be very small in torsional systems [4]. The inertias of the shafts and coupling are also neglected. The gears also have stiffness but the values are usually very large that it is safe to neglect them. If including it is important, a general relation can be used to estimate their stiffness [2]. The torsional stiffness, K, of a rotor element can be determined using K=GJ/L, where G is the shear modulus for the material of the rotor, J is the polar moment of inertia about the principal axis, which for a circular rotor can be written as $\pi D^4/32$, with D being the shaft diameter, and L is the length of the shaft. For a hollow rotor, J is given by $\pi(D_0^4-D_i^4)/32$, where D_o is the outer diameter and D_i is the inner diameter. If a shaft element is subjected to a given torque, T, and is twisted by an angle θ rad as a result, then K=T/θ. θ is usually determined using FEA.

For shaft elements connected in series, the effective stiffness, K_{eff}, can be calculated using:

$$\frac{1}{K_{eff}}=\frac{1}{K_1}+\frac{1}{K_2}+\ldots\ldots\ldots+\frac{1}{K_N} \qquad (2)$$

At a given gear stage that consists of a gear wheel and a pinion or a wheel, an idler and a pinion, the effective or combined inertia can be determined. If I_w is the wheel moment of inertia, I_p the moment of inertia of the pinion and I_d the moment of inertia of the idler, then for the case without an idler we can write: $I_{eff}=I_w+i_{wp}^2 I_p$, where i_{wp} is the gear ratio between wheel and pinion (ratio of number of teeth on wheel to number of teeth on pinion=G_w/G_p). If the wheel is first connected to an idler and the idler to the pinion, then $I_{eff}=I_w+i_{wd}^2 I_d+i_{wp}^2 I_p$, where $I_{wd}=G_w/G_d$. Adding an idler does not change the overall step-up between the wheel and the pinion. That is $i_{wp}=i_{wd} \times i_{dp}=(G_w/G_d) \times (G_d/G_p)=G_w/G_p$.

2.1 Amplification factor

If the natural angular torsional frequeny is denoted by ω_n and the forced response angular torsional frequency by ω, then according to reference [5], we can write:

$$\frac{\theta}{\theta_0} = \frac{1}{1\text{-}\left(\omega/\omega_n\right)^2} \qquad (3)$$

Plotting θ/θ_0 versus ω/ω_n gives three possible outcomes, namely, $\omega/\omega_n<1$, $\omega/\omega_n=0$ and $\omega/\omega_n>1$. The second outcome means that the relative angular deflection is infinitely large, which is seldom possible in physical systems because of the presence of damping. In this work, we are operating on the left of the line $\omega/\omega_n=1$. That is, $\omega/\omega_n<1$. The ratio $\frac{1}{1-\left(\omega/\omega_n\right)^2}$ gives an indication of the amplification of the shear stress or torque in the shaft element at resonance and is referred to as the amplification factor.

2.2 Motor torque

The electric motor used in this work is a 4 pole asynchronous motor. Between 1000rpm to 1500rpm, the torque is steady with some fluctuation about the rated torque and from 1500rpm to 1800rpm, the torque decreases. In general, $\omega=2\pi f$ and $f=np/60$, where n is the rotational speed of the drive in rpm and p is the number of pole pair. For a four poles motor, p=2, so we get $\omega=4\pi n/60$. The expression for the motor torque can therefore be written as:

$$T(t)=\begin{cases} T_1+T_0\sin\left(4\pi nt/60\pm\alpha\right), & 1000<n<1500rpm \\ 60P_0/2\pi n, & n>1500rpm \end{cases}, \qquad (4)$$

where T_1 is the rated torque, T_0 is the torque excitation amplitude, α is the phase angle and P_0 is the rated power of the motor. T_1 and T_0 are obtained by using time series data from measurement.

3. Torsional models development

The torsional models developed are done using the Holzer method [4], [5]. It is used because it can handle both branched and unbranched drive trains. When the relative angular deflection is not critical, the matrix Eigenvalue method can be used to determine the natural frequencies in both cases. But when the relative angular deflection is to be precisely determined then the Holzer method or the transfer matrix method are used for branched systems [5]. This is the case because two important boundary conditions must be satisfied. They are as follows: At the branched point, the torque entering must equal that leaving and the relative angular deflection of the branches entering the junction must be equal at the branched point. Two cases are considered here,

which are representative of the compressors analysed. The equivalent or reduced models are shown Fig. 3(a) and (b). Raw inertia values and stiffness values are used to compute the speed reduced inertia and stiffness depicted in the equivalent models.

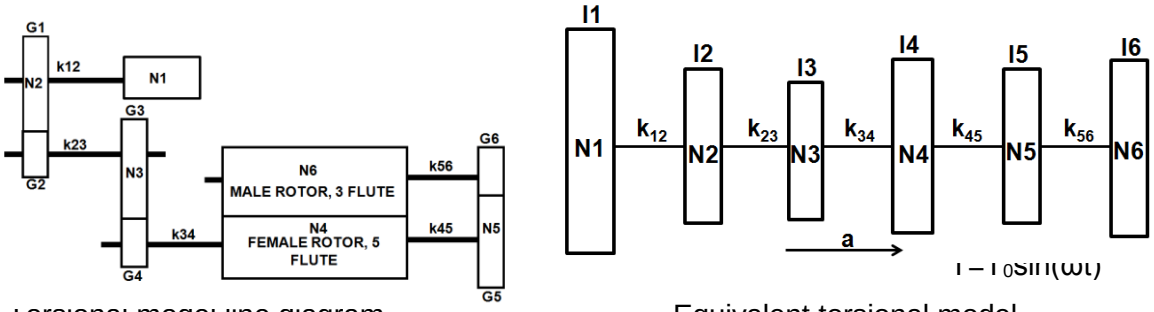

Torsional model line diagram Equivalent torsional model

(a) Drive train of twin screw compressor, no branching (Machines MK1 and MK2)

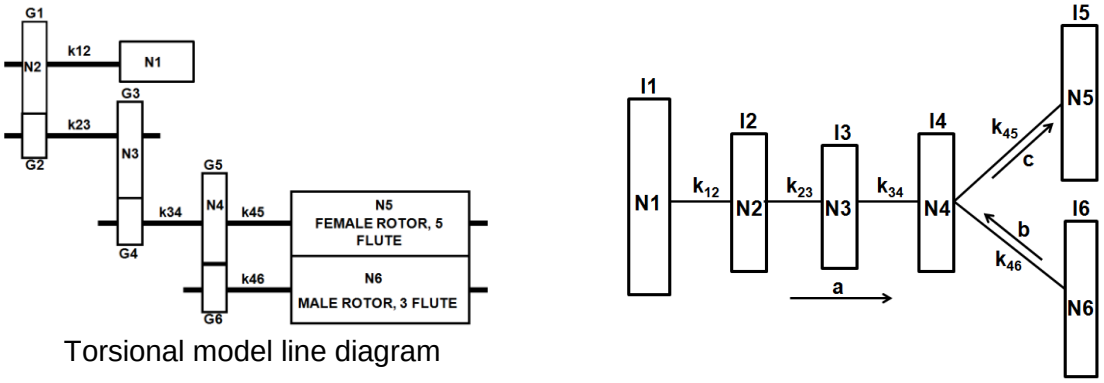

Torsional model line diagram

(b) Drive train of twin screw compressor with a single junction and branching (Machines MK3, MK4 and MK5)

Fig. 3: Equivalent torsional models of twin screw compressor without and with branching

MK1 is the new machine developed to replace the MK4 machine. It can be operated in both clockwise and counter clockwise directions. This is achieved by using an idler. The housing is also redesigned to enable it to fit on the 6x2 chassis of the truck. The MK2 is a variation of the MK1 that enables the input shaft to be off-set and by so doing reduce the input torque fluctuation. This is achieved by re-profiling the gear casing and the bearing carrier. The MK3 machine is a slight variation of the MK1 that is obtained by moving the synchronization gears to the drive side. Finally, the MK5 machine is the high speed version of the MK4 machine. Its input speed range is 2300rpm to 3300rpm. All other machines have an input speed range of 1000rpm to 1800rpm.

The drive train in Fig. 3(a) has two gear stages and a synchronization gear stage. N denotes the nodes, with N_1=Electric motor, N_2= Input gear stage, N_3=Second gear stage,

N_4=Female rotor, N_5=Synchronization gear stage, and N_6=Male rotor. The rotors used here have a 3/5 lobe combination and the main drive is through the female rotor. I_1=Motor inertia, I_2=First stage gear inertia, I_3=Second stage gear inertia, I_4=Female rotor inertia, I_5=Synchronization gear inertia and I_6=Male rotor inertia. For the torsional stiffness, K_{12} is the equivalent stiffness of the prop-shaft and the input shaft, K_{23} is the equivalent stiffness of the shaft element connecting the first stage pinion to the second stage wheel, K_{34} is the equivalent stiffness of the element between the second stage pinion an the centre of mass of the female rotor, K_{45} is the equivalent stiffness between the centre of mass of female rotor and the wheel of the synchronization gear stage and K_{56} is the equivalent stiffness between the pinion of the synchronization gear and the centre of mass of the male rotor.

Similarly, in Fig. 3(b), there are three gear stages as in Fig. 3(a) in the MK3 machine. The synchronization gear stage is on the drive side (Node 4) and the main drive is still through the female rotor. At the junction, the torque entering is distributed through both rotors. Also, at the junction, $\theta_{4a}=\theta_{4b}$. The drive trains in the MK4 and MK5 have only a single gear stage and a synchronization gear stage.

Applying the Holzer method to Fig.3(b) and for the free torsional models, the relative angular deflections at nodes 1 and 6 are assumed to be unity. That is $\theta_1=\theta_6=1$. Next, we begin with branch “a” and compute the relative angular deflection at node 4 (denoted as θ_{4a}) and then take branch “b” and also compute the relative angular deflection at node 4 (denoted by θ_{4b}). As boundary condition $\theta_{4a}=\theta_{4b}$. If this is not true, make $\theta_6=\theta_{4a}/\theta_{4b}$ in order to make the relative angular deflections at the junction equal. Next, we move to branch “c” and compute the residual torque (Te) at node 5 and this must be zero. The values of the angular frequencies (ω) for which Te=0 are the natural torsional frequencies of the system [5]. The same procedure above is repeated for the model in Fig. 3(a), but with no branching at node 4. Both models are implemented in MathCAD.

The forced torsional models are developed by applying the forcing torque, T, at node 2. Details of how the Holzer method is applied can be found in [6].

4. Results and discussions

Results of free and forced torsional vibration are presented and this is followed by sensitivity analysis of the stiffness and inertia. The results and discussions are proceeded by the conclusions and future outlook.

4.1 Free torsional vibration and validation with measurement data

Free torsional models of MK1, MK3, MK4, and MK5 are developed and their relative angular deflections are compared as shown in Fig. 4. In the absence of forced torsional models, this enables the prediction of the natural torsional resonance frequencies and the torque trend in the various machines, which can be compared with the measured torsional frequencies and torque trend.

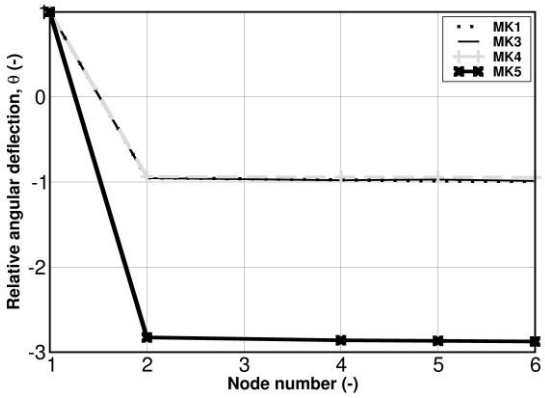

Fig. 4: Mode shapes of 1st torsional mode

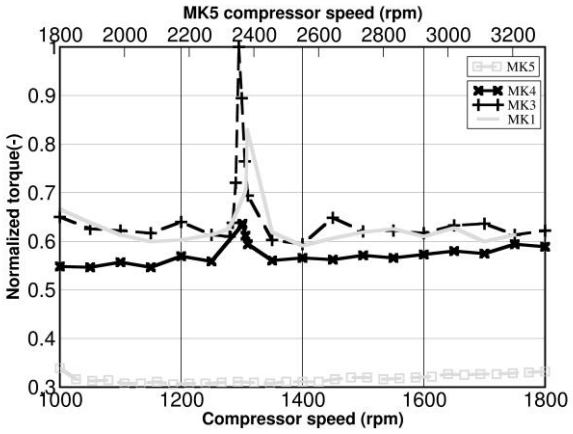

Fig. 5: Measured normalized torque peak

The models predictions of the relative angular deflections are: MK5>MK3>MK1>MK4 as presented in Fig. 4. From measurements, the torque peak trend is MK3>MK1>MK4>MK5 (See Fig. 5). The trend is good, with the exception of MK5, which shows almost no torque peak at the 1X input speed. This is because the torsional mode is not excited at the IX input speed in this machine. Fast Fourier Transform (FFT) of the MK5 torque data shows a fundamental mode with maximum response at the 2X input speed (See Fig. 12).

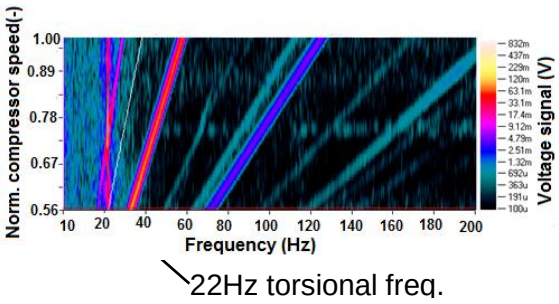

Table 1: 1st torsional frequencies

Machine type	Predicted first torsional freq. (Hz)	Measured first torsional freq. (Hz)	Amplification factor (-)
MK1	23.36	22.00	9
MK3	22.73	21.75	12
MK4	22.52	21.67	13
MK5	31.65	29.00	6

Fig. 6: MK1 waterfall plot

The reason for this is discussed in details under forced torsional models. Waterfall plots of torque (torque run-up spectrum) of the various machines showed resonance at 1X input speed, with the exception of the MK5. In this case, a faint line is seen at 29 Hz (1740 rpm), which is outside the speed range of this machine. A typical plot is shown in Fig. 6 for the MK1 machine. All the torques in Fig. 5 are normalized by the maximum torque measured in the MK3 machine. They are also measured using the same prop-shaft angle to enable comparison.

The measured and predicted first mode torsional frequencies are also in good agreement both in trend and magnitude (See Table 1). The mode shapes shown in Fig.4 indicates that the entire compressor is behaving like a rigid body that is moving relative to and out of phase with the electric motor. This makes it possible to model the entire compressor with the drive as a two point mass system, thus reducing greatly the computational time required to determine the first torsional modal frequency. The angular frequency in this case can be determined using:

$$\omega_1^2 = \frac{K_{eff}(I_1+I_2)}{I_1 I_2} \qquad (5)$$

Where K_{eff} is the equivalent stiffness of the prop-shaft and the input shaft located between the motor and the first stage input gear, I1 is the motor moment of inertia and I2 is the moment of inertia of the compressor drive train. Applying this to MK1, we get a first torsional frequency of 23.59Hz, which is close to the value predicted in Table 1.

A measure of the torque and hence shear stress in a shaft element is given by the gradient of line connecting the nodes that define that element in the drive train. That is tan(β_1) or tan(β_2). The most sensitive elements in Fig. 4 are therefore the elements connected between nodes 1 and 2 (That is, the prop-shaft, coupling and the input shaft). The maximum torque is expected to be in these elements as seen from the torque measurements.

4.2 Forced torsional vibration results and validation with measurement data

To enable the actual quantification of the torque and hence the shear stress in the input shaft and other shaft elements in the drive train forced torsional models are developed for the MK1 and MK2 machines. The latter machine is a slight variation of the former. In the latter the gear casing and bearing carrier are modified in order to offset the input shaft and by so doing reduce the prop-shaft angle and hence the input torque fluctuation. Comparing the torque peaks in MK1 and MK2 would quantify the effect of the prop-shaft angle reduction on torque peak. The MK1 prop-shaft angle, normalized by using the maximum prop-shaft angle is 1 while that of MK2 is 0.6, representing a reduction of 8° in the angle. The aim of the forced torsional model is to see if it can predict the torque peak reduction that has been captured in measurements. To develop the models curve fitting is used to determine the torque forcing function, T(t), using the electric motor torque time series data. The corresponding angular deflections in the shafts and the twisting moments are determined and compared with measurement data. The sampling rate of the torque time series data is 10kHz and a total of 10000 data points are taken at their 1X critical input speeds (1229rpm for MK1 and 1268rpm for MK2). The time step, Δt=1/(Sampling rate)=1x10^{-4} s. The torque is measured at the motor shaft using a torque transducer. The normalized time series data of both machines is depicted in Fig. 7, with the values plotted for 0.5 seconds of the total time of 2 seconds and normalized by the maximum torque measured in the MK1 machine. In Fig. 8, an FFT plot of the measured torque in both machines is presented.

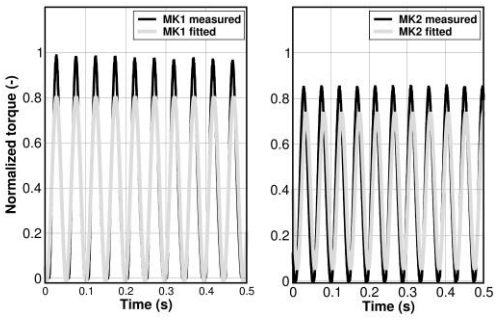

Fig. 7: Normalized torque time series (Expt. & fitted)

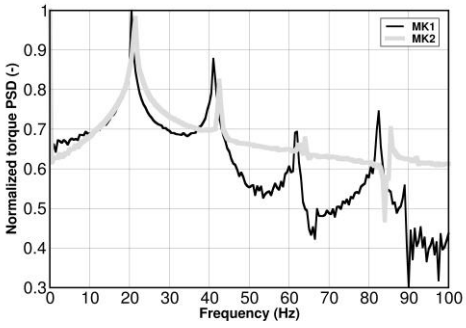

Fig. 8: FFT of measured torque

The power spectra density (PSD) of the torque is obtained using 20log10(T_{abs}), where T_{abs} is the absolute torque obtained from the FFT of the torque time series. It is normalized using the maximum value of MK1. In both cases in Fig. 8, maximum torque amplitude is occurring at the IX input speed (20.5Hz for MK1 and 21.5Hz for MK2), but the amplitude of

MK1 is higher than MK2, as expected. The normalized torque forcing function of MK1 and MK2 are $T_n(t)$=-0.404sin(128.805t+π/3)+0.3956 and $T_n(t)$=–0.3394sin(135.088t)+0.3951, respectively. The mode shapes obtained from the MathCAD implemented forced torsional models are shown in Fig. 9. From this figure, it can be seen that the angular twisting in MK1 is more severe than in MK2 due to the larger torque fluctuation in the former. The prediction of the actual torques in each shaft section makes it possible to determine the shear stress using $\tau = TR/G$, where τ is the shear stress and R the shaft radius.

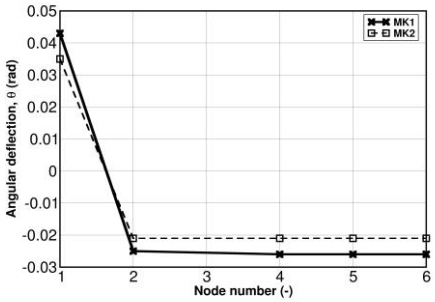

Fig. 9: Mode shapes (Predicted)

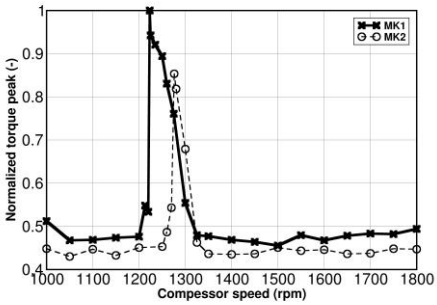

Fig. 10: Measured normalized torque

The model predicts a reduction of 124Nm in torque amplitude while the measurement is predicting a reduction of 122Nm in torque (See Fig. 10), which gives a percentage error of 1.6%. When the time series of torque is taken at non-critical speeds (for example, 1800rpm), the 2X input speed dominates (See Fig. 11). The 2X input speed torque peak is present at all speeds because the input shaft is connected to the prop-shaft via a coupling and the torque as a result cycles twice per shaft revolution. This 2X input speed peak is also present in the noise and vibration data of all the machines. The torque functions obtained also indicate that we have torque reversal (negative torque) at the 1X input speed, indicating that the compressor is attempting to drive the electric motor. This situation is undesirable as it can lead to backlash at the gears and gear noise and eventual damage of the machine, if it is left unchecked. To prevent this, some applications use springs at the input shaft to smoothen the input torque. Anti-backlash gears, for example, gears loaded with springs can also be used.

At a non-critical speed, for example, 1800rpm, the forcing function determined for MK1 is $T_n(t)$=0.175sin(376.99t)+0.804 and that for MK2 is $T_n(t)$=0.0877sin(376.99t)+0.797. In both cases, the torque amplitude and steady torque are normalized by the maximum torque measured in the MK1 machine. The forcing functions in these cases have positive torque amplitude, indicating there is no torque reversal at this speed. The coefficient of t in the general torque equation (4), ω=4πn/60, is obtained only when the input speed, n, is non-

critical. For example, when a non-critical speed of 1800rpm is considered, this value is 376.99rad/s. The same value is obtained when the measured time series data is fitted to determine the torque function, $T_n(t)$, given above at this speed. However, for say MK1 at 1229rpm critical speed, you get $\omega=4\pi n/60=257.40$rad/s=2X input speed and not 1X input speed obtained in the determined torque equation.

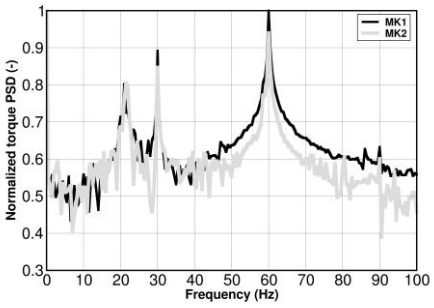

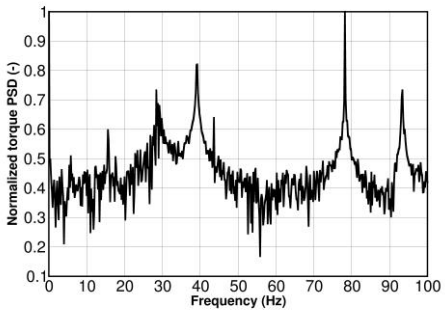

Fig. 11: Torque FFT of MK1 & MK2(Measured) **Fig. 12**: Torque FFT of MK5(Measured)

At 1800rpm (or 30Hz) for MK1 and MK2, the 1X input speed is not excited and so machine is not in resonance. In Fig. 11, FFT of the torque time series data of both machines at this speed is presented and clearly, the fundamental frequency (dominant mode) is at 60Hz=2X input speed and not 1X input speed. The same is true of the MK5 machine running at 2340rpm (or 39Hz) input speed. The FFT plot in Fig. 12 shows that the dominant frequency is 78.2Hz=2X input speed and not 1X input speed, thus avoiding the excitation of the first torsional mode. This explains why the torque peak measured in this machine is negligible when compared to the other machines in Fig. 5. In all the cases reported in Figs. 11 and 12, the torque amplitude at the IX input speed corresponds to the first sub-harmonic.

4.3 Sensitivity analysis

To determine the effect of changing the inertia (I) and stiffness (K) on the system response, sensitivity analyses is performed. In the case of the former, it is observed that the most sensitive element in the drive train is the male rotor followed by the female rotor. The mode shapes obtained when the raw inertia values are increased by a factor 1 to a factor 1.8 are shown in Fig. 13. As I is increased, the gradient, tanβ, decreases by 10% between β1 and β2 indicating a reduction in the relative angular deflection of the shaft element between nodes 1 and 2. The corresponding first mode torsional frequencies obtained are plotted in Fig. 14. Note that $\omega\sim1/I^{1/2}$ and $f=\omega/2\pi$ and so as I increases f decreases. When the inertia is decreased, the relative angular deflection is increased (in this case the gradient

increases by 39% from β1 to β2) and the first torsional frequency increases (See Figs. 15 and 16).

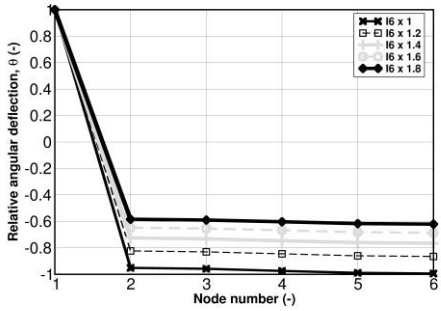

Fig. 13: Mode shapes (I_6 in MK1 increased)

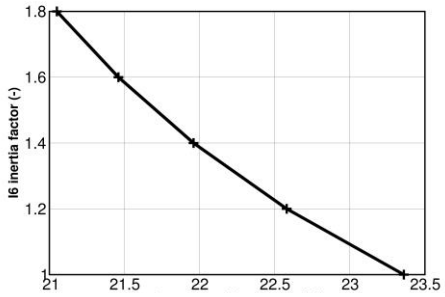

Fig. 14: 1st torsional freqs. (I_6 increased)

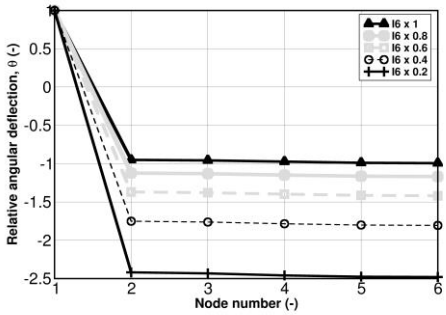

Fig. 15: Mode shapes (I_6 in MK1 decreased)

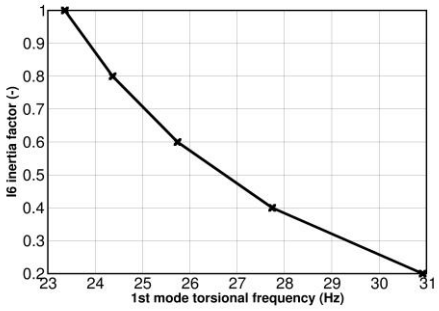

Fig. 16: 1st torsional freqs. (I_6 decreased)

A compressor with a larger rotor mass (larger diameter) will therefore have a lower torsional response when compared to a compressor with a smaller rotor mass (smaller diameter).

Sensitivity analyses of the stiffness of various shaft elements are carried out. It is observed that the prop-shaft stiffness has the most effect on the torsional response. In Fig. 17, the raw stiffness of the prop-shaft is increased by a factor 2 to 10 and the relative angular deflection changes as a result. The same is true of the first torsional frequencies obtained as in Fig. 18.

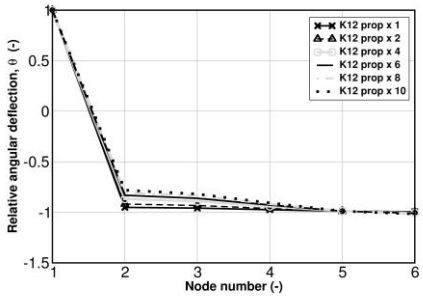

Fig. 17: Mode shapes (K_{12} in MK1 increased)

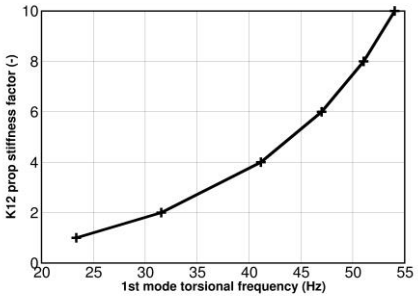

Fig. 18: 1st torsional freqs. (K_{12} increased)

This finding is implemented by tuning the prop-shaft to a stiffness that gives a first torsional frequency of 32Hz. In this case, no resonance is reported as the 32Hz (1920rpm) is outside the input speed range. When the stiffness of only the input shaft is increased by a factor of 2 to a factor of 10, no change in relative angular deflection is reported. The same is true of the other elements inside the machine (See Fig. 19). The corresponding changes in the first torsional frequencies are also marginal (See Fig. 20).

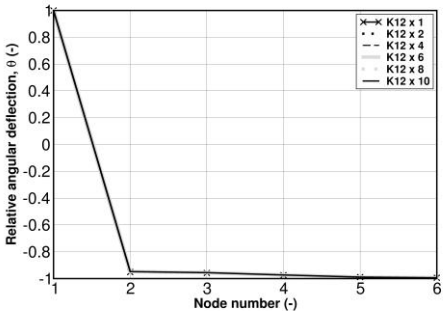

Fig. 19: Mode shapes (K_{12} in MK1 increased)

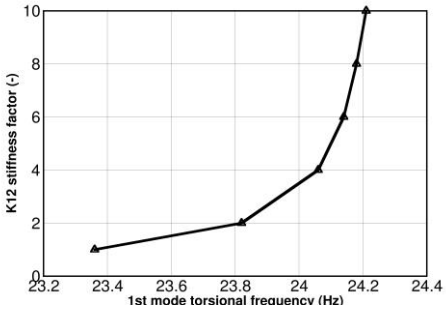

Fig. 20: 1st torsional freqs. (K_{12} increased)

5. Conclusions

Torsional analyses (free and forced) of dry screw compressors are presented. This is followed by sensitivity analyses of the inertia and stiffness of the elements in the drive train. The following conclusions can be drawn: (a) The source of torque peak increase in the drive train is identified as torsional and not structural. (b) The free torsional models developed show a good trend in relative angular deflection when compared to the torque measurements of MK1, MK3, and MK4. The only exception is the MK5. (c) Torque peaks predicted by the forced torsional models are in good agreement with those measured for the MK1 and MK2 machines. (d) Torque functions showed there is torque reversal at 1X critical input speeds (f) From the torsional stiffness standpoint, the most sensitive element in the drive train is the prop-shaft (g) The male and female rotors inertias in the drive train have more effect on the relative angular deflection.

6. Acknowledgment

The authors are indebted to the Gardner Denver team based at their DRUM facility in Bradford, UK, where all the measurements are carried out. We are particularly grateful to Steve Munt and Chris Witkowski, who did the measurements.

7. References

[1] Smith, D.R.:" Pulsation, vibration, and noise issues with wet and dry screw compressors". Proceedings of the Fortieth Turbomachinery Symposium, September 12-15, 2011, Houston, Texas.

[2] Leader, M.E., Kelm,R.D.: "Practical implementation of torsional analysis and field measurement". Technical Report.

[3] Feese, T., Maxfield,R.: "Torsional vibration problem with motor/ID fan system due to PWM variable frequency drive". Technical Report.

[4] Yuwen Y.: "Analysis of Multi-Branched Torsional Vibration for Design Optimization". Dissertation Submitted to the College of Engineering and Mineral Resources at West Virginia University in Partial fulfilment of the requirements for the degree of Doctor of Philosophy in Mechanical Engineering, 2004.

[5] Den Hartog, J.P.: "Mechanical Vibrations". Third Edition, McGRAW-Hill Book Company, INC, 1947.

[6] Glover, G.K.: "Mechanical Vibrations", Third Edition, NEM CHAND & BROS ROORKEE (U.P.), 1977.